8.2 AN OBJECTIVE SATELLITE-BASED TROPICAL CYCLONE SIZE CLIMATOLOGY

John A. Knaff and Mark Demaria
NOAA/NESDIS – Regional and Mesoscale Meteorology Branch
Fort Collins, Colorado

Scott Longmore
Cooperative Institute for Research in the Atmosphere
Colorado State University
Fort Collins, Colorado

Charles R. Sampson
Naval Research Laboratory
Monterey, California

1. Introduction

Tropical Cyclones (TCs) occur in many regions around the globe including the North Atlantic, eastern North Pacific, western North Pacific, North Indian Ocean and the Southern Hemisphere. There are many agencies that issue advisories, warnings and forecasts of these systems. The typical advisory contains information about individual TCs location, movement, intensity (in terms of maximum winds, and minimum sea-level pressure), and in many places radii of significant wind radii (gale-force, destructive and hurricane-force winds). Much of the focus of research has concentrated on motion and intensity, but it is the overall TC size in terms of wind field that often determines tropical cyclone impacts (e.g., Powell and Reinhold 2007, Houston et al. 1999) and areal coverage and distribution of rainfall (e.g., Kidder et al. 2005, Matyas 2010).

Past studies of TC size have shown that the intensity in terms of maximum winds is poorly related to the structure of the wind field beyond 1 degree latitude (111km) of the center, but the winds between 1 and 2.5 degree latitude of the center are well correlated with the radius of gales (R34, hereafter) (Weatherford and Gray 1988, Chan and Chan 2012). Correspondingly there is also a good relationship between the Radius of Outer Closed Isobar (ROCI) and the tangential wind profile of hurricanes (Merrill 1984). Others have shown that the initial size is often roughly maintained as the TCs intensify (Cocks and Gray 2002,Dean et al. 2009, Lee et al. 2010), that the size as measured by the R34 tend to increase during extra-tropical transition (Brand and Guard 1979) and when TCs become sheared, experience synoptic scale warm air advection and undergo eyewall replacement cycles (Maclay et al. 2008). Finally the small sizes of TCs that form close the equator (Brunt 1969) in the eastern North Pacific (Knaff et al. 2007) and midget typhoons that occur at subtropical latitudes (Arakawa 1952, Brand 1972, Harr et al 1996) have been documented.

Most of past studies, however, have been conducted in the western North Pacific or North Atlantic TC basins, and have used differing definitions of size based on either ROCI or R34, and in many cases the number of years and cases has been limited by data records. The studies of Merrill (1984), Chan and Chan (2012) and Lee et al. (2010) are among the most comprehensive studies to date. Merrill (1984) used ROCI as a size metric 1957-1977 (Atlantic) and 1961-69 (western North Pacific), and both Chan and Chan (2012) and Lee et al. (2010) used QuikSCAT surface wind estimates 1999-2009, and 2000-2005, respectively. These latter studies use wind speed thresholds that equivalent to R34 as a size metric. Unfortunately, to date no global TC size climatology has been created.

As mentioned previously past studies have relied upon the R34 and ROCI as size metrics and while it is has been shown that these two metrics are related they are not the same. These measures also have a number of shortcomings that make climatological studies difficult. In most cases R34 and ROCI are subjective estimates made from what data is available at the time of estimate and are subject to the actual method used to arrive at the best estimate, the notable exception are R34 estimated objectively from normally scarce observations. The use of the 34 kt wind threshold also precludes studies of weaker TCs with maximum winds below this threshold. Additionally, asymmetries in the wind field can cause additional issues when estimating a mean R34 as discussed in DeMuth et al. (2006). Finally the ROCI, besides being a subjective and method dependent, is also a function of the pressure field/environment in which a TC is embedded. For instance the ROCI could be infinite for a stationary storm if the environment were the same everywhere, but could also shrink solely due to accelerations in motion caused the mean flow.

For the reasons stated previously we endeavor to create a TC size metric that can be applied in a uniform manner globally over a long period of record to assess the climatology of TC size and compare to the previous studies. We also define TC size as the radius at which the TC influence on the near-surface wind field is indistinguishable from that of the environment, much as Dean et al. (2009). To do this we employ historical records of TC location, digital infrared (IR) imagery and large-scale environmental diagnostics of TCs to develop an algorithm for TC size and apply it to the global TC records to form a more complete climatology of TC size. The following sections discuss the data sets used, algorithm development, the results and discussion of our study.

2. Data Description

Infrared satellite information

For this study we make use of the brightness temperatures (T_b) from three-hourly storm-centered infrared (IR) imagery from the global constellation of geostationary satellites. The sources of these images come from two archives. The first is the Hurricane Satellite (HURSAT, Knapp and Kossin 2007) data version 3. This data set provides storm-centered IR window (with wavelengths of ~11μm) T_b on an 8 km x 8 km Mercator grid for global tropical cyclones starting in 1978 and ending in 2006. The second infrared data set comes from the Cooperative Institute for Research in the Atmosphere (CIRA) tropical cyclone IR image archive (referred to as the CIRA IR archive hereafter), which contains 4-km IR window observations of TCs that have been remapped to this resolution on a Mercator projection from various geostationary data platforms as described in Mueller et al. (2006). The CIRA IR archive, which has a higher temporal and spatial resolution, is used here to extend HURSAT v3 through 2011 at the same three-hourly temporal resolution.

a. TC track and intensity information

The track and intensity information used in this study comes from two sources. The first, for the period 1978-2006 (i.e., for the HURSAT cases), is contained in the HURSAT data files. That information is provided by the International Best Track and Archive for Climate Stewardship (IBTrACS, Knapp et al. 2010) The second source which is used to estimate storm centers and intensity for the 2007-2011 period (i.e., for the CIRA IR archive cases) is provided by the databases of the Automated Tropical Cyclone Forecast (ATCF; Sampson and Schrader 2000). These contain the final best track information produced by the National Hurricane Center, the Central Pacific Hurricane Center, and the Joint Typhoon Warning Center, who all utilize the ATCF. For this study will use the native ATCF units for TC intensity, which are knots (kt; 1kt = 0.514 ms^{-1}).

b. Large-scale TC diagnostics

For algorithm development we make use of the large scale diagnostic fields used to develop the Statistical Hurricane Predictions Scheme and the Logistic Growth Model (DeMaria et al 2005, DeMaria 2009). In particular we make use of the estimates of 1) azimuthal mean tangential wind at 850 hPa and at 500 km radius and 2) the vorticity at 850 hPa and at 1000 km radius. Both of these quantities are calculated from GFS model analyses. The 850-hPa azimuthally average tangential wind at 500 km is the quantity we utilized to estimate TC size. The 850-hPa vorticity is used to estimate the azimuthally averaged tangential wind at 1000-km, which is used for scaling our estimates of TC size. Specific details of how these are used to create an objective measure of TC size and scale that estimate to a measure of distance are described in the next section.

3. Methods and Scaling

a. Processing IR images

Three-hourly IR imagery were used to create storm centered polar analyses of T_b with 4-km radial spacing and 10-degree azimuthal spacing. The domain of these analyses is 600 km in radius. The storm centers provided in the HURSAT data set are used for these polar analyses of HURSAT imagery. For the CIRA IR archive, storm centers were estimated from the nominal times of the images the six-hourly positions in the best track using a cubic spline. The polar analyses are created using the variational analysis technique described in Mueller et al. (2006), but smoothing constraints were chosen so that the half-power wavelengths of the filter were 10 km in radius and 22.5° in azimuth.

To significantly simplify the problem of relating IR imagery to TC structure we then take azimuthal averages of the resulting polar T_b analyses, standardize those profiles at each radius (removing the sample radial mean and dividing by the sample radial standard deviation) and then perform a principle component analysis. Figure 1 show the leading modes of variability or empirical orthogonal functions (EOFs) along with the percent variance explained by each mode. EOF 1 is associated with the mean cloud top temperatures (radial wave number zero). EOFs 2 and 3 are related to radial structure of T_b and are related to radial wave number 1 and 2. These first three EOFs explain more than 95% of the variance. Principle components are then created for each three-hourly image in our combined HURSAT and CIRA IR archive dataset. In essence this procedure simplifies the problem from 150 azimuthal averages to three principle variables that explain the majority of the radial structure of T_b.

b. TC size algorithm development

For this study we use the azimuthally averaged tangential wind speed at 500 km radius as a proxy for TC size. There are several reasons for using this metric instead of the traditional metrics of ROCI or R34. The first justification is that the traditional metrics have significant shortcomings, as described in the introduction. The second justification comes from Frank (1977) who found that there is a "moat" region where moderate subsidence occurs below 400 hPa in rawinsonde composites and little if any deep convection occurs of typhoons. His work suggests that the convective portion of the storm is radially inside this moat region, but that the storm-induced tangential wind commonly extends beyond the 1550 km domain of his analysis. The third justification is that the mean tangential wind at a fixed radius is related to both the circulation and the vorticity via Stokes Theorem. This definition also allows the application of Kelvin's Circulation Theorem whereby the absolute circulation is quasi-conserved in the generally quasi-barotropic tropical atmosphere and outer regions of the TC. Also in the outer regions of a tropical cyclone circulation, which is characterized by low Rossby numbers and inertial stability, Coriolis accelerations are important. So in the outer regions of the TC, the mean tangential velocity at one radius should be well related to the mean tangential velocity at others and as the TC moves poleward the tangential wind at a fixed radius should decrease. Following this reasoning, the mean tangential wind at 1000 km should be close to half of its value at 500km. This also implies that there is some radius where the circulation measured at 500 km is close to the background flow. Furthermore, a similar strategy was successfully used to estimate TC size and provide improved wind-pressure relationships (Knaff and Zehr 2007). Finally, the current global models use advanced data assimilation and have resolution of global model analyses is sufficient to accurately estimate this metric.

In order to create an objective IR-based estimate of TC size, we use the 850-hPa mean tangential wind at r= 500 km (V500, with units of ms^{-1}) from the SHIP large-scale diagnostic files as the predictor of a multiple linear regression. The potential predictors for this regression are the sine storm latitude and the normalized principle components of the azimuthally averaged radial profiles of T_b from the center of the TC out to a radius of 600 km (i.e., associated with the EOFs shown in Figure 1). Previous studies have also shown that these EOFs can explain much of the symmetric of the TC vortex structure (Mueller et al. 2006, Kossin et al. 2007), further justifying this approach. A six-hourly subset of the Atlantic and East Pacific dependent sample 1995 to 2011 that contained data from the CIRA IR archive was used for initial algorithm development. The resulting multiple regression equation explains 29% of the variance of observed V500 and is based on the sine of the storm latitude and the first three normalized principle components, as shown in equation (1).

$$V500 = 2.488 + 11.478 * \sin\varphi - 1.350 * PC1 + 0.912 * PC2 + 0.319 * PC3 \qquad (1)$$

In equation (1) φ is latitude, and PC1, PC2, and PC3 are the normalized principle components associated with the EOFs shown in Fig. 1. Each predictor is statistically significant at the 99.99% using a two-tailed Student's t test. The positive coefficient associated with the latitude term implies that 1) TCs import more angular momentum than needed to maintain their current intensity and size, and 2) that baroclinic processes, which increase as the TC moves poleward, promote TC growth – echoing Merrill's (1984) statements. This term also implicitly includes effects related to viewing angle, and cloud top T_b increases with latitude. The negative coefficient on PC1 implies TCs with colder cloud shields (r=0 to r=600 km) tend to be larger. The positive coefficients with PC2 and PC3 are also consistent, suggesting colder cloud tops r=200 to r=600 km and r=70 to r=300 km, respectively are related to larger TCs.

Since the concept of TC size implies units of distance or area, we scale our regression equations that relate V500 to variations of latitude and IR principle components using the climatological (1995 to 2011) mean linear relationship between the circulation at 500 km (v500c) and at 1000 km (V1000c). Using the slope of this relationship and the estimated V500 we find the radius where the mean tangential wind is 5 kt (R5), which we consider a mean background flow, noting here that Dean et al. (2009) took a different approach. Thus for our study R5 is the radius of 5 kt positive tangential wind at 850 hPa that results from the TC circulation influencing a quiescent atmospheric environment. The relationship between V500 and R5 in units km is provided in equation (2), V500c=5.05 ms^{-1} and V1000c =2.25 ms^{-1}.

$$R5 = (952 + (V500 - V500c) * \frac{500}{V500c - V1000c}) \quad (2)$$

The values of R5 seem consistent Frank (1977) in that the tangential wind associated with the TC commonly extends beyond 14^{o} latitude (1550 km) radius of his analysis, noting that over 99% of R5 estimates are less than 21^{o} latitude (2330 km), but greater than 4^{o} latitude (440km). To make the units more manageable, for the remainder of this paper we will present R5 in terms of degrees latitude.

A reasonable question to ask is how is R5 (and/or V500) related to the radius of gale force winds? Using the same six-hourly developmental dataset used for algorithm development we relate the R5 based upon latitude and IR PCs to the azimuthally average of the non-zero operational 34-kt wind radii (R34) from the National Hurricane Center. For the combined eastern North Pacific and North Atlantic Sample R5 explains 30% of the variance of R34. However the region of the TC where gale-force winds are typically found is located between the core region of the storm where intensity determines the wind field and the outer part of the TC where R5 is an appropriate measure. Therefore it is expected that R34 is a function of both intensity (V_{max}) and R5/TC size. This is the case. When R5 and current intensity are used together they explain 38 % of the R34 variance, which is similar to results comparing scatterometer-based wind radii with those of the Joint Typhoon Warning Center in Lee et al (2010). The regression equation is provided in equation (3)

$$\underline{R34} = -98.63 + 1.33V_{max} + 28.19R5 \quad (3),$$

where V_{max} has units of kt and R5 has units of ^{o} latitude.

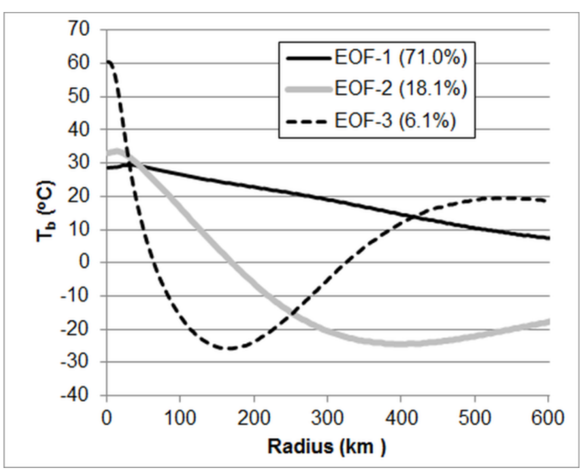

Figure 1. Leading modes of variability or Empirical Orthogonal Functions (EOFs) of the 6-hourly mean azimuthally averaged profiles of IR Tb. The percent variance explained by each EOF is shown in parentheses.

4. Results

In this section we present a basic climatology of R5 as a measure of the size of the TC vortex. Here we will describe the IR image composites of TC size as measured by the R5 metric, inter-basin TC size distributions, the mean lifecycle of TC size, spatial and seasonal distributions of large and small TCs, the spatial details of where TCs tend to grow the most/least, and finally the inter-annual trends of TCs size. Hereafter R5 and TC size will be used interchangeably.

a. IR Composites of TC size

Composite averages of IR imagery as a function of TC intensity and TC size were computed in order to show the utility of the R5 metric in discriminating TC size. Figure 2 shows the average of IR images for small, average, and large-sized TCs, which correspond to the 1-σ variations about the distribution of R5, which has a mean and standard deviation of 10.9 and 3.0^{o} latitude, respectively. The top panels across show the average IR image depiction of small (a), average (b) and large (c) TCs that have intensities less than 34 kt (tropical depressions). The mean intensities for these composite images are 25, 25, and 27 kt, respectively. The figure shows the composite images for small and average-sized storms are fairly symmetrical with the area with T_b colder than -20 ^{o}C being roughly twice as large for the average-sized composite. The large composite is characterized by larger and cooler T_b patterns with a central warm spot. The second row of Fig. 2 (d-f) shows the images associated with tropical storm-strength TCs (34-63 kt), with average intensities of 43, 46, 48 kt, respectively. These are similar to the tropical depressions, but the range of temperatures is larger. The average and large composites show signs of slightly smaller T_b features with the central features becoming noticeably cooler. The next row, Fig. 2g-i, shows the average images of minor TCs (64-95 kt) with mean intensities of 76, 77 and 79 kt, respectively. Here the range of cool temperatures continues to increase and a slight shrinking of contour features is evident as the core region consolidates. An eye feature is evident in the average composites. The final row (j-l) of Fig. 2 shows the major TCs (>95 kt) composite images with mean intensities of 108, 113, and 118 kt. In this row there is clear evidence of the existence of the TC eye at all sizes. Again the T_b in the composites increases from the minor TC composites shown in the row above. The small TC composites of major and minor TCs shows generally warmer T_b within 100 km of the TC center.

Figure 2 provides the reader a visual reference for the gross variability of IR features explained by the R5 metric. For small and average sized TCs the region with T_b less than -20 ^oC appears nearly the same as the TC intensifies from depression to major hurricane. The large composite show the same behavior for the area colder than -40 ^oC. In general the R5 metric appears well related to the sized of the overall size of the T_b pattern; suggesting the deep convection free "moat region" of Frank (1977) varies with R5. One interesting feature in the composites is the suggestion that R5 values are not well related to eye sizes, but rather are well related to the width of the cold cloud ring surrounding the eye, especially in the major hurricane composites. Such differences would impact satellite-based intensity estimates made using the Dvorak Technique (Dvorak 1984), suggesting a potential cause of the Dvorak positive intensity biases associated with large major TCs (via the ROCI) reported in Knaff et al. (2010). It is noteworthy however, that large TCs can have very large eyes whereas the eye size of smaller storms are limited by their overall smaller scale.

Since the identification of TCs with intensities greater than or equal to 34 kt is less ambiguous than weaker TCs and because more intense storms are of greater interest, the remainder of the paper will discuss results associated with TCs with 34 kt or greater intensity.

b. Inter-basin distributions

Using the R5 metric we now investigate the TC size distributions as a function of TC basin. Figure 3 shows the frequency distribution of R5 in the North Atlantic, eastern North Pacific, western North Pacific, North Indian, and Southern Hemisphere TC basins as a function of storm intensity. Frequencies are again provided for tropical storms (34-63kt), minor hurricane/typhoon (64-95 kt), and major hurricane/typhoon (>95 kt) intensity samples. The use of tropical storm, minor and major hurricane/typhoon/TC to describe these intensity ranges will be used hereafter. Table 1 contains the number of cases in each intensity range, along with the mean R5, intensity, and latitude of each subsample.

The North Atlantic R5 frequency (Fig. 3a) shows the size progression with intensification which is seen in all the basins. It also shows that the range of R5 for tropical storms is wider than the other basins, save for the North Indian Ocean, which has but a few cases. Table 1 shows that this basin also has the largest mean latitude of all the basins, which contributes to the relatively large mean sizes. There is also evidence that this basin can produce rather large major hurricanes. The major hurricane frequency distribution is slightly skewed toward larger sizes.

The R5 frequency in the eastern North Pacific (Fig. 3b) shows that this basin produces the smallest TCs of the basins examined and that the TCs in this basin only grow slightly with increasing intensity. This result is similar to those of Knaff et al. (2007) which showed the climatological 34-kt wind radii are about a third smaller in the eastern North Pacific when compared to the North Atlantic. The latitudes associated with these samples, however compare well with those of the Southern Hemisphere, suggesting that latitude is not the sole cause of this distribution. Rather it appears that the eastern North Pacific forms small TCs that generally do not move much further poleward and do not appear to grow much with intensification. The frequency distribution for tropical storms is skewed toward smaller sizes.

The distribution of R5 in the western North Pacific is narrower for all intensities when compared to the Atlantic, with the North Pacific producing on average larger tropical storms minor and major typhoons. The size distribution of the major typhoons does appear to be slightly larger, but more peaked than those of the other basins, despite those typhoons being located at significantly lower latitude than major hurricanes in the Atlantic. So it appears that the western North Pacific generally produces the largest most intense TCs, which agrees with conventional wisdom. The North Indian TC basin (Fig. 3d) contains only a fraction of the global TC activity. There are many more tropical storm intensity TCs in the record and the R5 distribution is noticeably different than the higher intensities. The few storms that become minor hurricane-strength produced a rather broad distribution of R5 with an indication of a bimodal nature. Many of the minor hurricane-strength TCs appear to intensify to major hurricane strength as they move poleward (Table 1) and grow; shifting the R5 distributions to larger sizes while maintaining the shape of the distribution.

Tropical cyclones in the Southern Hemisphere display R5 distributions (Fig. 3e) that are similar to those of the North Atlantic, but the distribution of major TCs is less skewed. However unlike the TCs of the N. Atlantic, TCs in this basin appear to develop and intensify in a rather narrow range of latitudes (Table 1). This suggests that the size distributions in this basin, while similar to the N. Atlantic, may be caused by different mechanisms.

c. TC growth lifecycle

In the previous section the frequency distributions of R5 suggested that TCs generally grow with increases related to changes in latitude, intensity, and time. In this section we examine the lifecycle of TC growth by stratifying the R5 statistic by the timing of the peak intensity, following Emanuel (2000), but further stratify the composites by the peak intensity ranges that the TC was observed to obtain (34-63 kt, 64-95 kt, >95 kt). Not only can we examine the lifecycle of R5, but since the latitude of each data point can be removed, we can examine the TC size changes that are not explicitly linked to latitude variation in the algorithm.

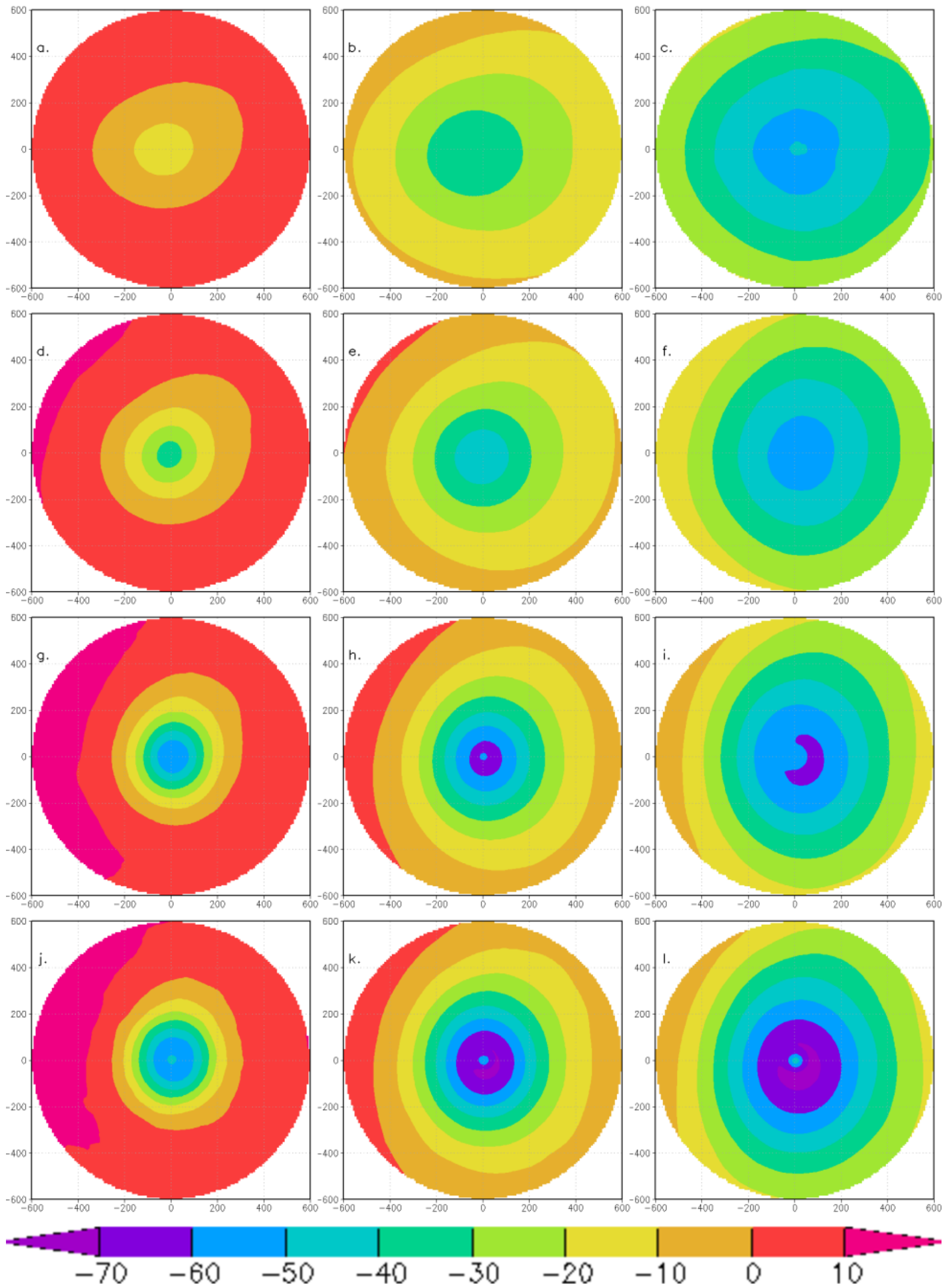

Figure 2. Composite average T_b for TCs with intensities < 34 kt (a-c), 34 to 63 kt (d-f), 64 to 95 kt (g-i), and >95 kt (j-l), and R5 sizes < 7.5 ^{o} latitude (a, d, g, and j), 7.5 to 12.45^o latitude (b, e, h, and k) > 12.45 ^{o} latitude (c, f, i, and l). The scale for T_b is provided at the bottom of the figure in units of ^{o}C.

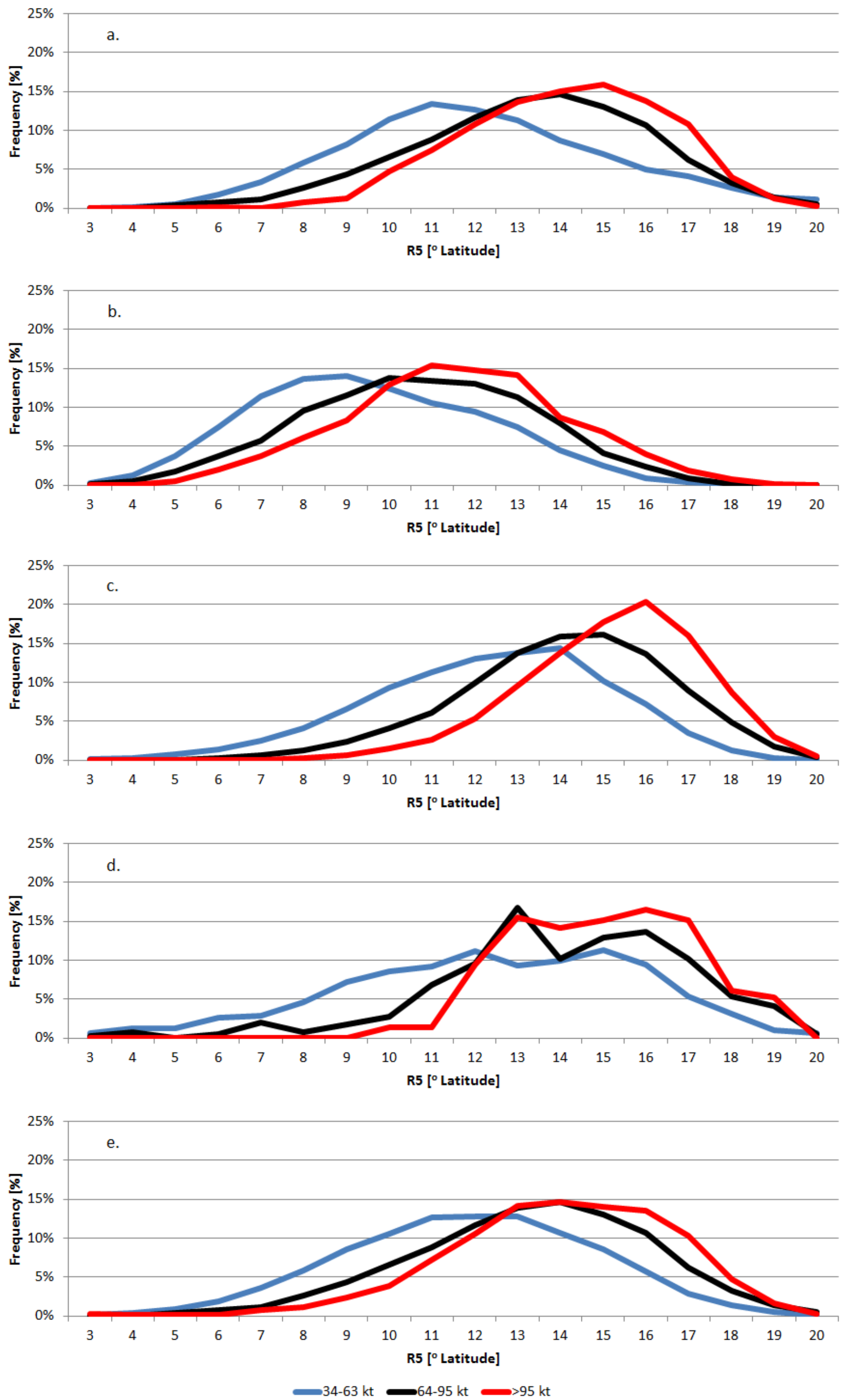

Figure 3. Frequency distributions of TC size (R5) for the North Atlantic (a), eastern North Pacific (b), western North Pacific (c), North Indian Ocean (d) and Southern Hemisphere (e) tropical cyclone basins. Blue lines, black lines, and red lines are associated with tropical storm, minor hurricane, and major hurricane intensities as indicated in the key (see text for additional information).

Table 1. Statistics associated with Figure 4. Shown are the intensity category, the number of cases, the mean R5, intensity (V_{max}) and latitude. The units for R5 and V_{max} are ^{l}atitude and kt, respectively.

Intensity Category	Cases	R5	V_{max}	Latitude
North Atlantic				
Tropical Storms	10900	11.7	46.2	28.0
Minor Hurricanes	4802	13.1	76.3	28.2
Major Hurricanes	1649	13.6	115.1	22.1
Eastern North Pacific				
Tropical Storms	11429	9.1	45.6	16.9
Minor Hurricanes	5779	10.2	77.5	17.7
Major Hurricanes	2790	11.1	113.9	16.4
Western North Pacific				
Tropical Storms	17141	11.8	46.5	20.3
Minor Typhoons	9910	13.6	78.0	21.4
Major Typhoons	5472	14.7	117.4	19.6
North Indian Ocean				
Tropical Storms	2457	11.8	43.8	14.3
Minor TCs	395	13.4	75.4	15.7
Major TCs	212	14.5	114.2	18.2
Southern Hemisphere				
Tropical Storms	18178	11.4	45.0	-17.3
Minor TCs	6857	12.8	77.3	-17.6
Major TCs	3140	13.5	112.4	-16.6

Figure 4 shows R5 (left) and the R5 metric with the latitude predictor in equation (1) removed (right) for tropical storms, minor TCs, and major TCs. Concentrating on the left half of this figure a few observations can be made. 1) TCs tend to grow as they intensify, and 2) the size of the TC well before maximum intensity is reached roughly determines the TC size at maximum intensity, and 3) the different basins seem to display both markedly different initial sizes and lifecycle evolution, particularly for the major TCs, 4) storms tend to shrink after peak intensity, save for in the North Atlantic.

When the influence of increasing latitude is not included in equation (1) (i.e., the right half of Figure 4) there are several observations. First the size TCs in the eastern North Pacific and Atlantic are initially comparable, but diverge after peak intensity. Second, there is some commonality between the size evolution of southern hemisphere and western North Pacific systems. There is also evidence that tropical storm-strength TCs do not grow much by factors other than those related to increasing latitude. This observation is also true for hurricane-strength systems in the eastern North Pacific and Southern Hemisphere. Much of the no-latitude-variation growth of minor typhoon and major typhoons occurs during and prior to maximum intensity, whereas the minor and major hurricanes in the Atlantic appear to continue to grow after maximum intensity is reached. This growth during weakening for Atlantic TCs has been documented in studies by Merrill (1984), Kimball et al. (2004) and Maclay et al. (2008).

d. Occurrence statistics of large and small TCs

In this subsection we examine the occurrence statistics of large and small TCs as measured by R5. Here we concentrate on minor and major-strength TCs as these are more important from an energy perspective and the results of tropical storm-strength systems are similar. Figure 5 shows the locations of the largest 25% and smallest 25% TCs at their first recorded maximum intensity. The top panel shows the location of maximum intensity of minor TCs. The majority of largest minor TCs occur in the North Atlantic and western North Pacific in regions where TCs typically recurve (see Figure 1 of Knaff 2009). The majority of the small minor TCs occur in the eastern North Pacific and elsewhere either in the northern hemisphere subtropics or at low latitude (equatorward of 20^{o}). This later observation agrees with Brunt (1969) statements suggesting that TCs at low latitude tend also to have small sizes. However there is also evidence of a few small minor typhoons occurring poleward of 20^o, which agree well with the locations of midget typhoons/very small typhoons documented in Arakawa (1952), Brand (1972) and Harr et al. (1996). A similar subtropical occurrence of very small minor hurricanes occurs in the North Atlantic. There is also an indication that small and large minor TCs that occur in the Southern Hemisphere are nearly equally distributed with larger storms tending to occur at slightly higher latitude and again in regions where TCs more typically recurve. It is also worth mentioning that the Bay of Bengal produces a few large minor TCs, but given this basin's typical activity and vulnerability to storm surge, this result is noteworthy.

The bottom panel in Figure 5 show the location of maximum intensity associated with TCs that reached intensities greater than 95 kt. These results are rather similar to the location of maximum intensity of minor hurricanes, but are generally shifted equatorward and are more concentrated in both the longitudinal and latitudinal directions, suggesting the importance of warmer oceanic conditions for the strongest TCs. It is noteworthy that both the Bay of Bengal and Gulf of Mexico, trapped TC basins known to be vulnerable to storm surge, produce a few large TCs with intensities greater than 95 kt. Large very intense TCs also seem to more common in La Reunion in the South Indian Ocean, Taiwan, Japan and China in the Western North Pacific, South Pacific, the United States of America, the Bahamas and Bermuda in the North Atlantic. There is again an indication of small major TCs occurring either in the eastern North Pacific or equatorward of 20^o (i.e. very few in the subtropics). However, it is noteworthy that equatorward of Australia small major TCs seem to predominate.

Figure 5 shows where the largest and smallest TCs typically occur. Furthermore, when the latitude term is not used, the distribution of small and large storms shown in Figure 5 does not appreciably change (not shown), which means that large TCs either begin as large storms (i.e., as implied in Figure 4) and/or they continue to grow following maximum intensity as is the case in the western North Pacific and North Atlantic composites also shown in Fig. 4. Section 4e will discuss TC growth tendencies further.

Where large and small TCs typically exist is important, but when small and large TCs form is also interesting. Unlike Figure 5, which shows global size quartiles, the results shown in Figure 6 are based upon basin specific quartiles.

Figure 6a, b shows the frequency distribution for small, large and all minor hurricanes and major hurricanes in the North Atlantic, respectively. Figure 6a shows some indication that small minor hurricanes peak earlier and have a little broader temporal distribution. Figure 6b shows that larger major hurricanes have tended to occur earlier in the season, particularly in August whereas small major TCs appear have had slightly higher frequencies in September and October. All and all the seasonality of TC size in North Atlantic is rather difficult to interpret without additional information.

Figure 6b, c shows the frequency distribution for small, large and all minor hurricanes and major hurricanes in the eastern North Pacific. In this basin small minor hurricanes have occurred more frequently later in the season whereas large minor hurricanes are most frequent very early in the season. The frequency distribution of small major hurricanes peaks in July and small major hurricanes appear more frequent in May, June and July. On the other hand, large major hurricanes in this basin occur later and are more frequent August – December and small major hurricanes occure earlier (May-July).

In the western North Pacific large and small typhoons (Fig 6d) have quite different frequency distributions. Large minor typhoons have occurred more frequently in the months of June-October and have distribution that is more peaked and appears to be associated with the months when the equatorial southwesterly flow (i.e., monsoon trough) is most common. Small minor typhoons occur more frequently both before and after the peak of the season (i.e., when the monsoon trough circulation is most common). Small major typhoons (Fig 6f) occur more frequently before and after the normal peak of activity and were particularly more frequent in the months of October, November, December, January, April and May. Large major typhoons are most frequent in July, August and September. These results agree well with similar findings presented in Brand (1972).

The frequency of large and small TCs in the Southern Hemisphere also seems to be related to seasonality of the equatorial northwesterly flow. Large minor and major TCs have been more common in the most active parts of the Southern Hemisphere TC season. Conversely small TCs appear to be most common in both the early and late portions of the season in the months of October, November, March, April and May.

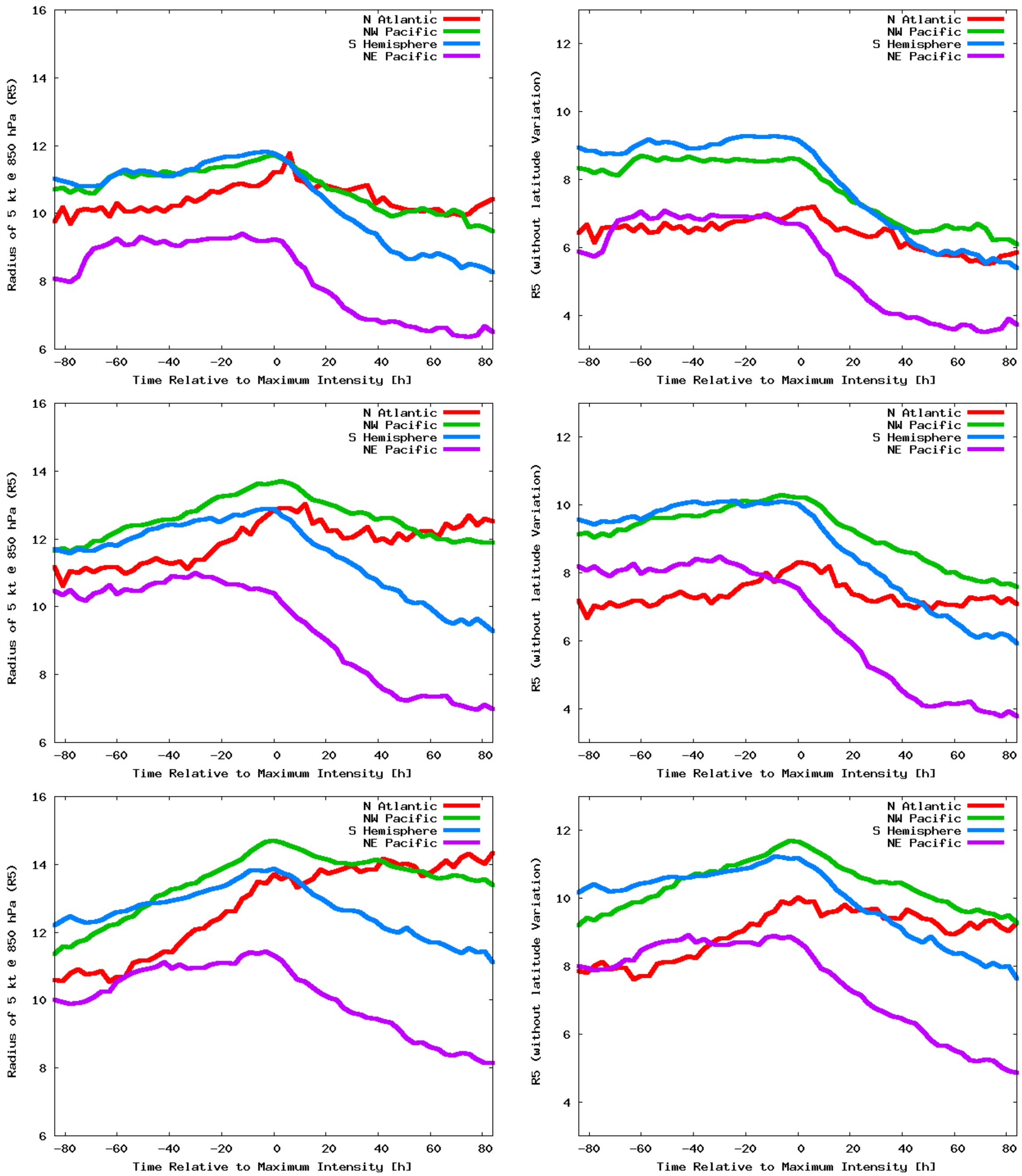

Figure 4. Composites of TC size (R5) based on the timing of maximum intensity (i.e., time = 0 h). For TCs in the intensity (V_{max}) ranges 34 kt ≤ V_{max} < 64 kt (top row), TCs with 64 kt ≤ V_{max} < 96 kt (middle row), and TCs with V_{max} ≥96 kt (bottom row). Panels on the left are of R5, and on the right are R5 calculated without the latitude contribution.

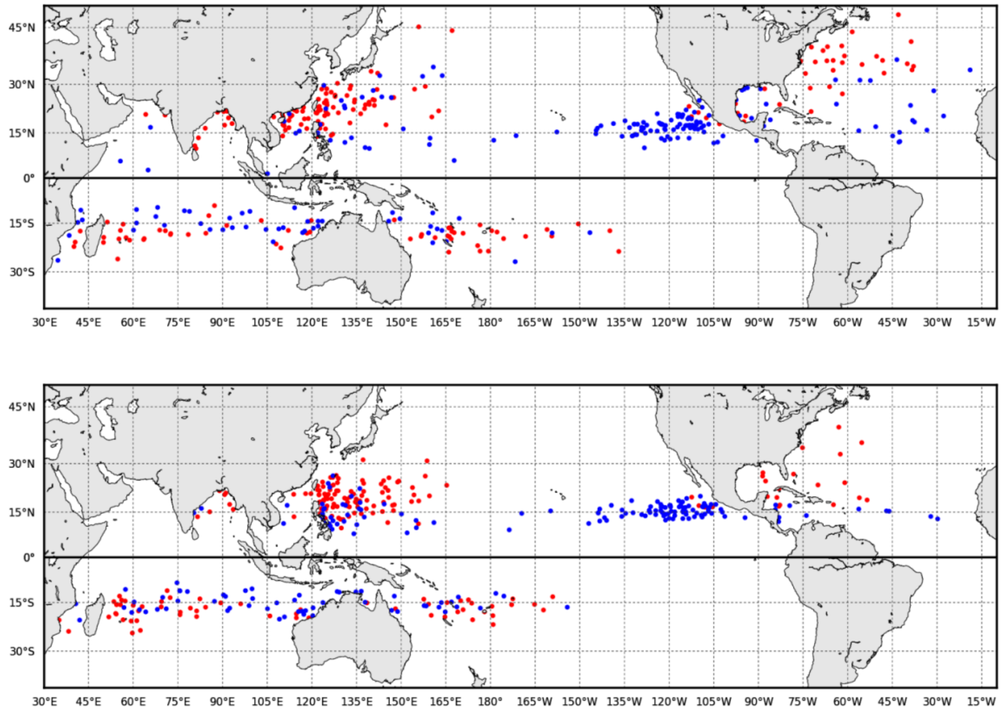

Figure 5. Locations of the largest (red) and smallest (blue) 25% of TCs based according to R5. TCs that reached minor hurricane intensity are show in the top panel and those that reached major hurricane intensity are shown in the bottom panel.

e. Growth tendencies.

Figure 7 (top panel) shows the tracks of the 10% fastest growing TCs following maximum intensity and remain hurricane-strength. The most frequent regions for post-peak intensity TC growth are the regions to the east of the major continental land masses of Asia, North America, Africa and Australia. From the tracks shown on Fig. 7, these episodes of rapid post-peak growth often occur in regions preferred for recurvature and extra-tropical transition. There is also a less evident suggestion that storms also have the tendency to grow following landfall over narrow landmasses (i.e., the Philippines, Yucatan Peninsula, Florida), somewhat disagreeing with Brand and Blelloch (1973), who examined typhoon structure following landfall in the Philippines, but only the 24-h following reemergence in the South China Sea.

Figure 7 (middle) shows the tracks of the 10% fastest shrinking TCs prior to attaining their maximum intensity and that remain at hurricane-strength. The storm tracks and tendencies are quite different. These the tracks of these pre-peak shrinking TCs appear are predominated by westward non-recurving TCs (eastern/western North Pacific, South Indian Ocean), but those that recurve appear to have obtained maximum intensity following recurvature or well before recurvature. Maximum intensity also usually occurs shortly after maximum size is obtained (less than a day).

Figure 7 (bottom) shows the tracks associated with those hurricane-strength TCs that reach both maximum intensity and size simultaneously. With the exception of the eastern North Pacific, TCs that display this behavior characterized by landfall nearly coincident with maximum intensity, rather erratic tracks which suggest weak steering, post recurvature maximum intensity and poleward and eastward motion. Frequent landfalling cases in this category occurred in Northern Australia, the South China Sea, the Gulf of Mexico, and the Bay of Bengal. The latter two track behaviors are often associated with less than ideal conditions for further intensification such as increased or constantly changing vertical wind shear, increased upper oceanic cooling associated with slow motion and lower sub-tropical ocean heat contents (Knaff et al. 2013). Erratic tracks in the subtropical regions typically correspond to the TC being *located in the center of the subsiding subtropical ridge.*

f. Trends in TC size

Since the combined effects of TC size and intensity (via increase kinetic energy) are related to hurricane damage potential (Powell and Reinhold 2007), trends of TC size (R5) from our dataset are also examined. And R5 is well related to R34 (section 2). TC size was examined in two ways. We examined the TC size at maximum intensity and the maximum TC size for storms having at least hurricane-strength intensity using basin specific quartiles and global quartiles. The trend results of TC size at maximum intensity and at maximum size were nearly identical; reiterating the results in Figure 4 that suggest the initial TC size is well related to the future size evolution. For that reason only the trends of maximum size with intensities greater or equal to 64 kt are shown in Figure 8. We also begin our TC size trend analysis in 1981; given that satellite data prior to that year is generally sparse in several TC basins.

Figure 8a shows the time series and trend of North Atlantic maximum hurricane size. The time series in the North Atlantic shows the R5 varies generally between values of 10 and 20 degrees latitude, but the intra-annual variation is generally large producing a fairly consistent scatter between these ranges between 1981 and 2011. The resulting trends are slightly negative over these years and not statistically significant. Figure 8b shows the maximum hurricane size time series in the eastern North Pacific. The size range in this basin has a smaller range; generally ranging between 6 and 17 degrees latitude, with a few exceptions. As was the case in the North Atlantic, 1981-2011 trends are slightly negative and are not statistically significant. The time series of maximum typhoon size is shown in Fig 8c. The maximum size of typhoons in the western North Pacific varies roughly between 9 and 21 degrees latitude. Trends of maximum typhoon size are slightly positive, but again are not statistically significant. Much like the western North Pacific hurricane-strength TC size in the Southern Hemisphere (Fig 8d) is confined to a range of R5 with values generally between 9 and 21 degrees latitude. The trends of TC size in the Southern Hemisphere are also found to be slightly negative, which again lack statistical significance. It is not surprising that the global trends of TC size of hurricane-strength TCs is essentially zero and lacking statistical significance), is dominated by storm-to-storm variability, and does not show any obvious signs of any relationship with known tropical inter-seasonal variability. The reader is also directed toward Knutson et al. (2010) and references within for research related to current and future trends of TC intensity, and precipitation.

5. Discussion

The objective IR-based TC size metric, R5, allows for an objective examination of the global TC size climatology including size distributions, typical evolutions, spatial distributions, seasonal tendencies, typical locations and tracks associated with growth and trends. These results appear to agree with many of the results of past studies where ROCI and R34 were used as size metrics and that concentrated on the North Atlantic and western North Pacific TC basins. Below we will summarize our findings and relate them to past studies, where applicable. This will be followed by a discussion about new findings and future research.

The basin specific distributions of TC size (Fig. 3) showed that North Atlantic and western North Pacific TC basins produce some of the widest ranges and largest TCs with the western North Pacific producing the largest TCs. The Atlantic distribution of major hurricanes is broader with larger ranges of R5. The eastern North Pacific basin produces the smallest TCs. The North Indian Ocean basin, which has but a few cases, has a broad size distribution for minor and major TC size, with many major TCs becoming very large as they move poleward and grow. The Southern Hemisphere R5 distributions are similar to those of the North Atlantic. It appears, as expected from previous work by Merrill (1984) Chan and Chan (2012), that TCs that maintain hurricane-intensity and move poleward through the sub-tropics tend to grow, but there is clearly differences between the distributions suggesting that different physical mechanisms may be promoting TC growth more in some basins (North Atlantic, western North Pacific) and less in others (eastern North Pacific).

When TCs were composited with respect to the occurrence of the (first) maximum intensity to examine the typical evolutions with respect to intensification and weakening several features became evident (i.e., Fig. 4). First the eastern North Pacific produces noticeably smaller TCs. There is also evidence that tropical storms do not grow much by factors other than those related to intensification. This observation is also true for minor TCs in the eastern North Pacific and Southern Hemisphere. Minor TCs in North Atlantic; however appear to continue to grow even after maximum intensity. This appears to be the case for major TCs in this basin too. The mean post-peak intensity evolution of TC size in the western North Pacific seems to be somewhere in between the behavior found in the North Atlantic and the eastern North Pacific.

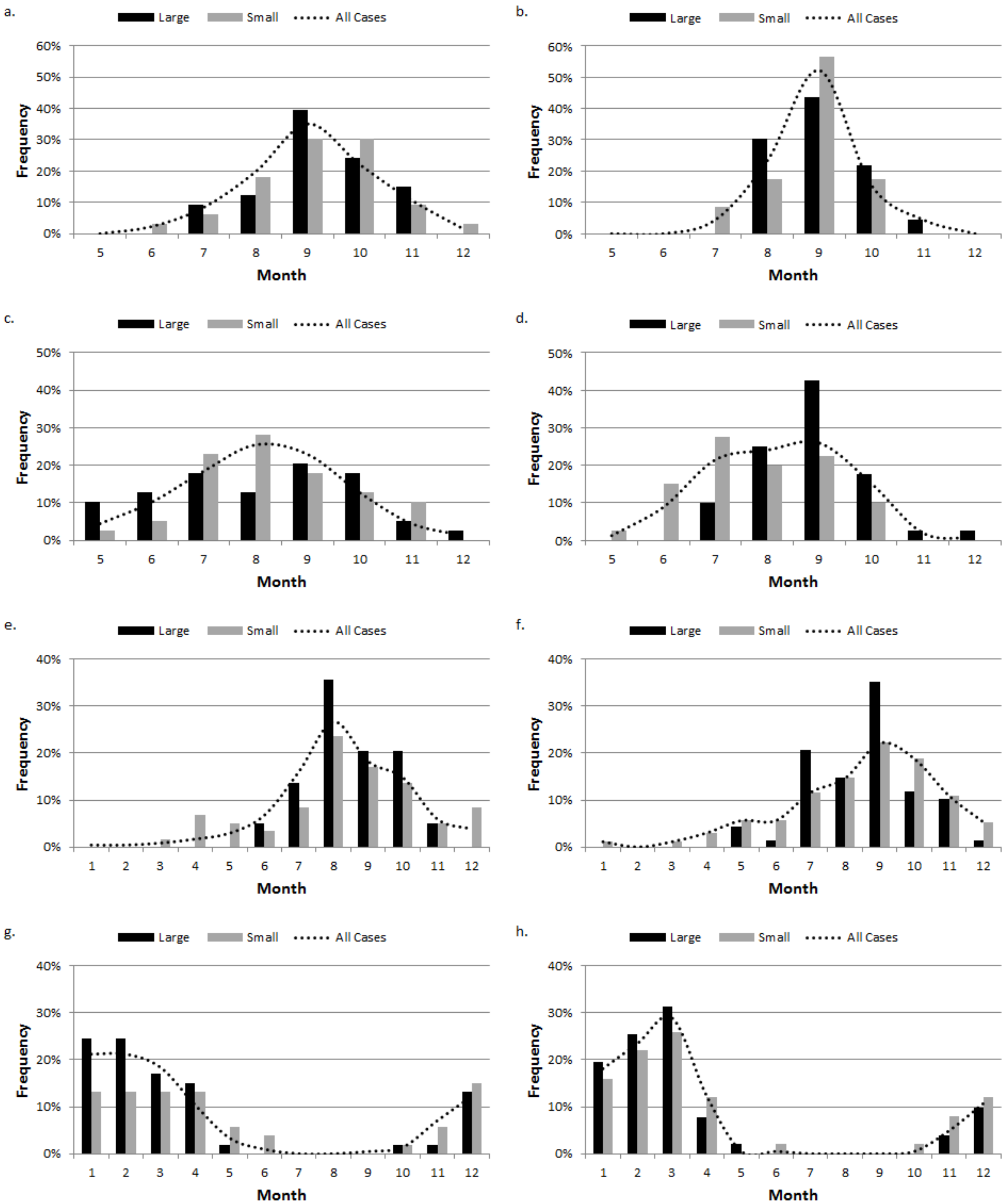

Figure 6. Monthly frequency diagrams of TC size. Large and small TC frequencies are shown along with the typical frequency of all storms. The left panels (a, c, e, and g) are for minor hurricanes and the right panel (b, d, f, and h) are for major hurricanes. Results are based on the lower (small) and upper (large) quartiles in each basin. Results from the North Atlantic (a, b), eastern North Pacific (c, d), western North Pacific (e, f) and the Southern Hemisphere (g, h) are shown.

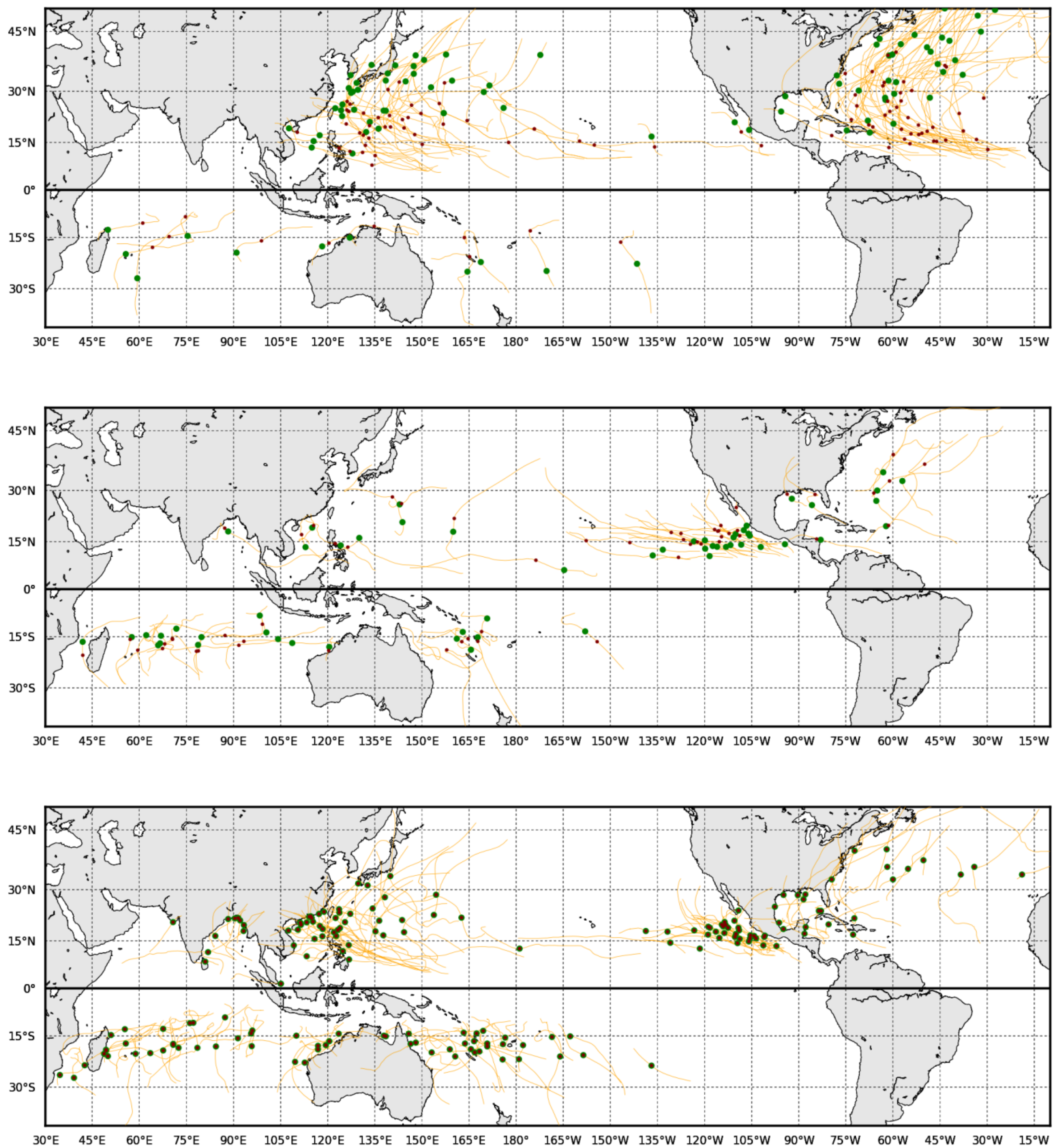

Figure 7. The illustration shows tracks of the post-maximum-intensity, quartiles of the fastest growing (top) and slowest growing (bottom) TCs with intensities greater than 63 kt. The TC tracks (yellow), points of maximum intensity (maroon) and points where the hurricane-strength system is the largest (green) are provided on the figure. Results are based on cases 1978-2011.

Thus, in the eastern North Pacific and Southern Hemisphere, and to a lesser degree in the western North Pacific, there is evidence that major TCs grow during the intensification phase and shrink as they weaken when the factors related to increasing latitude are removed. Removing the latitude influence from our regression shows that behavior of TCs in all the basins, save the North Atlantic, is rather similar. However, it shows that the latitude of the TCs in the eastern North Pacific cannot explain the tendency for small TCs there. So it appears that much of the no-latitude-variation growth of minor typhoon and major typhoons occurs during and prior to maximum intensity, whereas the stronger TCs in the Atlantic appear to continue to grow after maximum intensity is reached. This growth during weakening for Atlantic TCs has been documented in studies by Merrill (1984), Kimball et al. (2004) and Maclay et al. (2008).

A few general findings about TC size evolution can be made. TCs tend to grow as the increase in latitude, agreeing with Merrill (1984). TCs tend to grow the most as they intensify. The size of the TC well before maximum intensity is reached is well related to the TC size at maximum intensity, agreeing with the conclusions of Cocks and Gray (2002) and Lee et al. (2010). Finally, the different basins seem to display both markedly different initial sizes and lifecycle evolution, particularly for the major TCs. This may be the result of climatological differences in baroclinicity and vertical wind shear between the basins, factors previously related to TC growth (Brand and Guard 1973, Maclay 2008). It is worth noting that westerly shear would impart a positive circulation tendency, whereas easterly wind shear would promote a negative circulation tendency. Our TC size estimate methodology can be used to examine such speculation.

The upper and lower quartiles of TC size were compared for the minor and major TC samples (Fig. 5). There is clearly a suggestion of preferred locations for large and small storms. The majority of largest minor and major TCs occur in the North Atlantic and western North Pacific in regions where TCs typically recurve. The majority of the small minor and major TCs occur in the eastern North Pacific. Small Minor TCs are also found to occur at sub-tropical latitudes– agreeing with the locations of midget typhoons (Arakawa 1952, Brand 1972 and Harr et al. 1996), and suggesting possibly unique formation mechanisms. Small major TCs, while still occurring most often in the eastern North Pacific, exclusively occur elsewhere at low latitude (equatorward of 20^{o}) – agreeing with Brunt's (1969) unreferenced observation that TCs at low latitude tend also to have small sizes. There is also an indication that small and large TCs in the Southern Hemisphere are nearly equally distributed with larger storms tending to occur at slightly higher latitude and again in regions where TCs more typically recurve. However, poleward of Australia small major TCs seem to predominate. It is also worth mentioning that the storm surge prone Bay of Bengal and the Gulf of Mexico have shown a tendency to produce relatively large and intense TCs.

One could argue that the result shown in Figure 5 is due solely to the use of latitude in the R5 algorithm. Furthermore, when the latitude term is not used, the distribution of small and large storms shown in Figure 5 does not appreciably change (not shown). Furthermore, the well distributed latitudinal results in the Southern Hemisphere suggest that other factors, particularly environmental changes associated with TC recurvature (i.e., more baroclinic environments) is also a key contributing factor. The results provided in the East Pacific also suggest that the environment in that basin is favorable for producing small TCs that stay relatively small. It is noteworthy that storms in the eastern North Pacific rarely recurve (Knaff 2009).

The seasonality of large and small TCs (i.e., Fig. 6) shows that in the eastern North Pacific the occurrence of small major hurricanes earlier in the season. These may possibly be in response to periodic warm El Nino/Southern Oscillation conditions that provide more favorable ocean conditions early in the season and at lower latitude. The higher frequency of large major hurricanes may be related to the relatively rare event of hurricanes recurving in this basin in late September, October and November. A similar seasonality is shown to occur in the Southern Hemisphere with small (large) storms occurring prior to and after (during) the typical peak of the season, which is more often associated with equatorial westerly flow and the existence of a monsoon trough pattern.

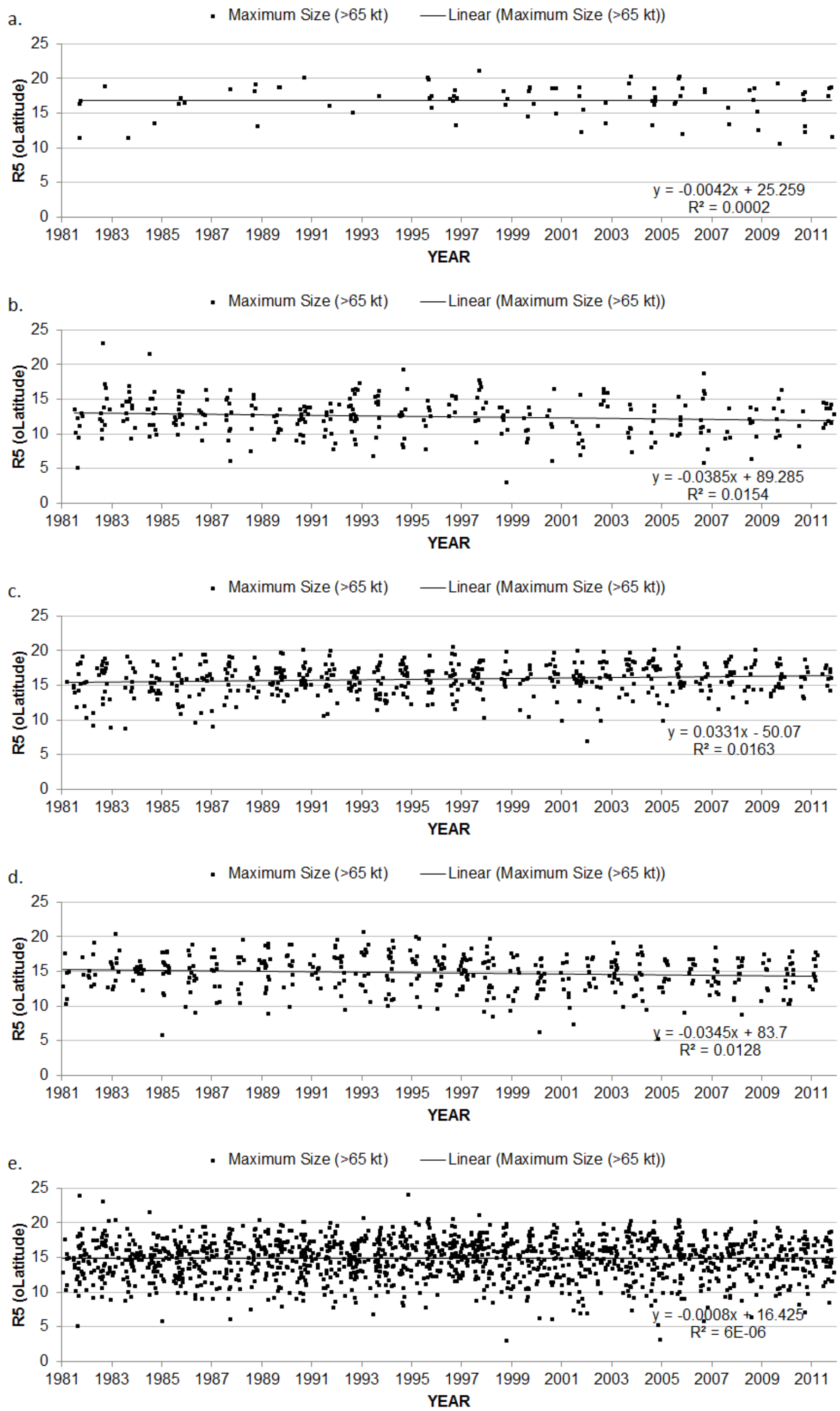

Figure 8. Time series of TC size (R5) for the North Atlantic (a), eastern North Pacific (b), western North Pacific (c), Southern Hemisphere (d) and Global (e) of TCs with intensities greater than 63 kt and occurring during 1981-2011 in our database. The individual TC values are shown along with a trend line (solid line). The regression equation and percent variance explained (R^2) are also provided for each panel.

In the western North Pacific, the higher frequency of larger typhoons near the peak of the season is suggestive that large TCs often form in association with the seasonal monsoon trough. Smaller TCs in this basin show tendencies that suggest they more frequently form in the pre- and post-monsoon periods. These finding reaffirm the Lee et al. (2010) results suggesting that the low-level environment determines the differences between large and small TCs. That is the monsoon trough (south westerly flow, monsoon shear, and converging northeasterly and southwesterly flow) leads to large storms and the other synoptic situations, particularly trade wind (easterly waves) and unclassified, lead to smaller TCs (see Lee et al. 2009, their Figure 7). These findings are also supported by Chan and Chan (2012, their Figure15) results who find larger mean R34 during the July – October are found to occur in El Nino years when the monsoon trough is more active and TCs typically have longer lifecycles.

In summary, it appears that in basins where the convergence of equatorward westerlies with trade winds flows (i.e., a monsoon trough) for a preferred region for TC formation (eastern North Pacific, western North Pacific and Southern Hemisphere), small storms are more frequent before and after the peak of the season and less frequent during the periods when the monsoon trough is most active. This suggests that large storms are more common when there are greater amounts of climatological synoptic scale relative vorticity/circulation as suggested by Lee et al (2010).

The largest growth occurs in regions of climatological baroclinicity where mid-latitude westerlies extend into the tropics and steer TCs poleward. Many of these TCs are shown to be recurving into the westerlies as they grow. TCs that shrink in size during intensification tend to move predominately westward or have tracks and behaviors associated with less favorable environments for intensification. TCs that simultainously experience maximum size and intensity tend to rapidly weaken either due to landfall or due to hostile environmental conditions.

Another finding that is not so obvious in Figure 7 is that there are few TCs that hit the Philippines close to the time of their maximum intensity and continue to move westward growing quite rapidly in the South China Sea. So there is some evidence that TCs grow as they re-intensify after they pass over narrow land masses. Brand and Blelloch (1973) examined Typhoons crossing the Philippines and found that the eye size increase following passage and the radius of outer closed isobar contracted in the first 24-hours after reemerging in the South China Sea. Their findings along with ours suggest that the post-Philippine-landfall growth of typhoons likely occurs more that 24-hours after reemerging over water. There is also some indication that similar physics may be occurring as storms pass over other narrow land masses (e.g., Yucatan Peninsula, Florida, Madagascar, the Arabian Peninsula).

The maximum TC sizes in all the basins examined show no significant inter-annual trends or much inter-seasonal variability. The later finding is different than that of Chan and Chan who found an ENSO signal in the average size of the July-October period. The locations (Fig. 5), the seasonality of large and small storms (Fig. 6) and the growth tendencies (Fig. 7), however agree quite well with their results. We on the other hand examine the trends in all seasons and for brevity sake did not examine sub seasonal variability.

Many of the findings of this study reconfirm past work in the North Atlantic and Western North Pacific as discussed above, but have put these in a global context. Results confirm that the propensity for large storms increase when storms form during seasons that are characterized by enhanced low-level vorticity, when storms move into environments characterized as increasingly baroclinic, especially after peaking in intensity prior to recurvature. This study confirms largest major TCs occur in the western North Pacific. As others have shown, small storms tend to form during seasons when low-level vorticity is provided by the incipient disturbance rather than the synoptic environment where the flow is often dominated by easterly trade winds, in the center of the subtropical ridge (as is the case with midget typhoons). Post-peak-intensity TC growth can also be halted by landfall and other rapid weakening.

New findings of this study include a clear indication that small major TCs predominate low latitudes. This study also allows for the direct comparison of size distributions between the individual TC basins. That is the eastern North Pacific produces smaller TCs whereas the western North Pacific, Southern Hemisphere and North Atlantic produce larger TCs. This study clearly shows there are preferred regions, seasons and track types for growth. Information about the lifecycle of TC growth with respect to the timing of maximum intensity is provided and leads to these findings 1) TCs tend to grow more as they intensify, and 2) the size of the TC well before maximum intensity is reached is well related to the TC size at maximum intensity, and 3) the different basins seem to display both markedly different initial sizes and lifecycle size evolutions, and 4) storms tend to shrink after peak intensity, save for in the North Atlantic. Furthermore this analysis clearly shows that the TCs of North Atlantic maintain their size after peak intensity with the Atlantic showing that stronger TCs continue to grow after peak intensity (i.e. results obtained from the Atlantic are not applicable everywhere). The equivalent in the other basins show storms tend to grow during intensification can even shrink after peak intensity. Finally the analysis of inter-annual trends of TCs with intensities greater than 63 kt show that over the last 30 years there have been no significant trends in this objective measure of TC size.

There is much future work that can utilize the dataset produced by this approach – which can be maintained as long as there are TC best tracks and geostationary satellite data. First is to improve the understanding of what environmental factors, beyond generalizations of vertical wind shear, baroclinicity etc., are responsible or related to TC growth. Such studies will make use of environmental diagnostics derived from numerical weather prediction analyses and other observational data. Such knowledge would lead to the development of techniques to better anticipate TC growth. These datasets can also be used for case studies of individual systems, especially those in the past, where traditional observations of size may be missing etc. Finally, these data can be used to for studies of the detailed inter-annual and intra-seasonal variability of TCs. We look forward to working on a few of these problems in the near future.

Acknowledgements: The views, opinions, and findings contained in this report are those of the authors and should not be construed as an official National Oceanic and Atmospheric Administration or U.S. government position, policy, or decision.

References:

Arakawa, H., 1952: Mame Taifu or midget typhoon (small storms of typhoon intensity). Geophys. Mag., 24, 463–474.

Brand, S., 1972: Very large and very small typhoons of the western North Pacific Ocean. *J. Meteorol. Soc. Japan.*, 50, 332–341.

Brand, S., J.W. Blelloch, 1973: Changes in the Characteristics of Typhoons Crossing the Philippines. *J. Appl. Meteor.*, **12**, 104–109.

Brunt, A.T., 1969: Low latitude Cyclones. *Aust. Met. Mag.*, 17, 67-90.

Cocks, S. B., W.M. Gray, 2002: Variability of the outer wind profiles of western North Pacific typhoons: Classifications and techniques for analysis and forecasting. *Mon. Wea. Rev.*, **130**, 1989–2005.

Dean, L., K.A. Emanuel, and D.R. Chavas, 2009: On the size distribution of Atlantic tropical cyclones. *Geophys. Res. Lett.*, **36**, L14803.

DeMaria, M., 2009: A simplified dynamical system for tropical cyclone intensity prediction. *Mon. Wea. Rev.* **137**, 68–82.

DeMaria, M., M. Mainelli, L.K. Shay, J.A. Knaff, J. Kaplan, 2005: Further improvement to the Statistical Hurricane Intensity Prediction Scheme (SHIPS). *Wea. Forecasting*, **20**, 531-543.

Demuth, J., M. DeMaria, and J.A. Knaff, 2006: Improvement of Advanced Microwave Sounding Unit tropical cyclone intensity and size estimation algorithms, *J. of App. Meteor. Clim.*, **45**, 1573–1581.

Dvorak, V.F., 1984: Tropical cyclone intensity analysis using satellite data. NOAA Tech. Rep. 11, 45 pp. [Available from NOAA/NESDIS, 5200 Auth Rd., Washington, DC 20333.]

Emanuel, K.A., 2000: A statistical analysis of hurricane intensity. *Mon. Wea. Rev*., **128**, 1139-1152.

Houston, S.H., W.A. Shaffer, M.D. Powell, and J. Chen, 1999: Comparisons of HRD and SLOSH surface wind fields in hurricanes: Implications for storm surge and wave modeling. *Wea. Forecasting*, **14**, 671-686.

Harr, P.A., M.S. Kalafsky, and R.L. Elsberry, 1996: Environmental conditions prior to formation of a midget tropical cyclone during TCM-93. *Mon. Wea. Rev.*, **124**, 1693–1710. doi:10.1175/1520-0493

Irish, J.L., D.T. Resio, and J.J. Ratcliff: 2008: The influence of storm size on hurricane surge. *J. Phys. Oceanogr.*, **38**, 2003-2013.

Kimball, S. K., Madhuri S. Mulekar, 2004: A 15-year climatology of North Atlantic tropical cyclones. Part I: Size parameters. *J. Climate*, **17**, 3555–3575.

Kidder, S. Q., J.A. Knaff, S. J. Kusselson, M. Turk, R.R. Ferraro, R. J. Kuligowski, 2005: The Tropical Rainfall Potential (TRaP) technique. Part I: Description and examples. *Wea. Forecasting*, **20**, 456–464.

Knaff, J.A., M. DeMaria, C.R. Sampson, J. E. Peak, J. Cummings, and W. H. Schubert, 2013: Upper oceanic energy response to tropical cyclone passage. *J. Climate*, in press. doi: http://dx.doi.org/10.1175/JCLI-D-12-00038.1

Knaff, J.A**.,** D.P. Brown, J.Courtney, G.M. Gallina, J.L. Beven II, 2010: An evaluation of Dvorak Technique-based tropical cyclone intensity estimates. *Wea. Forecasting*, **25**, 1362-1379.

Knaff, J.A., C.R. Sampson, M. DeMaria, T.P. Marchok, J.M. Gross, and C.J. McAdie, 2007: Statistical tropical cyclone wind radii prediction using climatology and persistence, *Wea. Forecasting*, **22**, 781–791.

Knapp, K.R., and J.P. Kossin, 2007: New global tropical cyclone data from ISCCP B1 geostationary satellite observations. *J. of Appl. Remote Sens.*, 1, 013505.

Knapp, K.R., M.C. Kruk, D.H. Levinson, H.J. Diamond, and C.J. Neumann, 2010: The International Best Track Archive for Climate Stewardship (IBTrACS): Unifying tropical cyclone best track data. *Bull. Amer. Meteor. Soc.*, **91**, 363-376.

Knutson, T.R., J.L. McBride, J. Chan, K. Emanuel, G. Holland, C. Landsea, I. Held, J.P. Kossin, A.K. Srivastava, and M. Sugi, 2010: Tropical cyclones and climate change. *Nature Geoscience*, **3**, doi:10.1038/ngeo779.

Lee, C.S., K.K.W. Cheung, W.-T. Fang, and R. L. Elsberry, 2010: Initial maintenance of tropical cyclone size in the western North Pacific. *Mon. Wea. Rev.*, **138**, 3207-3223.

Maclay, K.S., M. DeMaria and T.H. Vonder Haar, 2008: Tropical cyclone inner core kinetic energy evolution. *Mon. Wea. Rev*., **136**, 4882-4898.

Matyas, C.J., 2010: Associations between the size of hurricane rain fields at landfall and their surrounding environments. *Meteor. Atmos. Phys.*, **106**, 135-48.

Merrill, R. T., 1984: A comparison of large and small tropical cyclones. *Mon. Wea. Rev.,* **112**, 1408–1418.

Mueller, K.J., M. DeMaria, J.A. Knaff, J.P. Kossin, and T.H. Vonder Haar 2006: Objective estimation of tropical cyclone wind structure from infrared satellite data. *Wea Forecasting,* **21**, 990–1005.

Powell, M.D., and T.A. Reinhold, 2007: Tropical cyclone destructive potential by integrated kinetic energy. *Bull. Amer. Meteor. Soc*., **88**, 513–526.

Sampson, C. R., and A. J. Schrader, 2000: The automated tropical cyclone forecasting system (version 3.2). *Bull. Amer. Meteor. Soc.*, **81**, 1231–1240.